Nature of the $Si(SiMe_3)_3^+$ Cation in Aromatic Solvents

Carl-Henrik Ottosson and Dieter Cremer*,†

Department of Theoretical Chemistry, University of Göteborg, Kemigården 3, S-412 96 Göteborg, Sweden

Received March 7, 1996[⊗]

The silylium cation $Si(SiMe_3)_3^+$ (**1**) was investigated by HF, B3LYP, PISA-HF, SCRF, and the NMR/ab initio/IGLO approach in the gas phase and in benzene solution employing the 6-31G(d) basis set. In the gas phase, the $\delta(^{29}Si)$ value of the central Si atom of **1** is 920 ppm relative to that of TMS according to IGLO/[7s6p2d/5s4p1d/3s1p]//HF/6-31G(d) calculations, which is in line with the corresponding $\delta(^{29}Si)$ values calculated for other silyl-substituted silylium cations and results from large paramagnetic contributions to the $\delta(^{29}Si)$ shift value. In benzene solution, **1** forms the Wheland σ-complex $Si(SiMe_3)_3$-$C_6H_6^+$ (**3**), in which the silylium cation character of **1** is lost despite the fact that **3** is the weakest silylium cation−benzene complex so far investigated. According to NMR/ab initio/IGLO calculations, complex **3** is characterized by a weak covalent SiC bond of 2.293 Å, a coordination energy of 13.6 kcal/mol, and a $\delta(^{29}Si)$ value of 111 ppm. Steric blocking by three $SiMe_3$ groups is not sufficient to prevent a silylium cation from interacting with aromatic solvent molecules.

1. Introduction

In recent publications, it has been claimed that trivalent silylium cations SiR_3^+ can be generated in condensed phases.[1−3] These authors investigated trialkyl- and trisilyl-substituted silylium ions in toluene and benzene solutions as well as in the solid state. However, theoretical studies on several potential trialkylsilylium cations provide convincing evidence that SiR_3^+ ions form Wheland σ-complexes with aromatic solvent molecules and, accordingly, have to be considered as silyl-substituted carbocations rather than free silylium cations.[4−9]

There is still doubt about the electronic nature and the degree of solvent coordination in the case of the $Si(SiMe_3)_3^+$ cation (**1**) generated in aromatic solvents. Upon comparison to the precursor silane $HSi(SiMe_3)_3$ (**2**), which has a $\delta(^{29}Si)$ NMR chemical shift of −117.4 ppm at its central Si, the corresponding value for the alleged cation **1** in benzene solution is 111.1 ppm.[1a,b] A downfield shift of 228 ppm between **2** and alleged **1**, which is large compared to ^{29}Si shift changes for the corresponding trialkylsilyl cationic species (80−100 ppm),[1c] could indicate uncoordinated **1**. However, since different $\delta(^{29}Si)$ values are found for alleged **1** in benzene and toluene solutions,[1a,b] some kind of solute−solvent interactions should occur. The question is whether these interactions lead to a tetracoordinated Si compound with a covalent Si−C bond and, thereby, a loss of silylium cation character. So far, no theoretical investigations have been performed on a potential $Si(SiMe_3)_3-C_6H_6^+$ complex (**3**) to clarify this question.

To describe the nature of **1** in benzene solution, we investigated molecules **1** and **2** as well as the complex **3**. In addition, we carried out calculations on silylium cations SiH_3^+ (**4**), $SiH_2SiH_3^+$ (**5**), $SiH(SiH_3)_2^+$ (**6**), and $Si(SiH_3)_3^+$ (**7**) and the potential complex $Si(SiH_3)_3-C_6H_6^+$ (**8**) for reasons of comparison (Scheme 1). Complex **8** has also been investigated by Olah and coworkers,[5] and we will frequently refer to the results of these authors.

2. NMR/ab Initio/IGLO Method and Determination of Molecular Geometries

For an accurate description of **1** in benzene solution, we have applied the NMR/ab initio/IGLO method (IGLO:individual gauge for localized orbitals), which is perfectly suited for the determination of molecular geometries in solution.[10−12] The method is based on the sensitivity of calculated NMR chemical shifts with regard to the geometry used.[10−12] Previous investigations have shown that reasonable $\delta(^{29}Si)$ NMR chemical shifts are obtained if the geometry of the Si compound in question has been optimized at the Hartree−Fock (HF) or second-order Møller−Plesset (MP2) level using a DZ+P basis sets.[4−8] Since the calculated NMR chemical shifts clearly depend on the geometry, an agreement between experimental

† E-mail: CREMER@OC.CHALMERS.SE.

⊗ Abstract published in *Advance ACS Abstracts,* November 15, 1996.

(1) (a) Lambert, J. B.; Zhang, S. *J. Chem. Soc., Chem. Commun.* **1993**, 383. (b) Lambert, J. B.; Zhang, S.; Stern, C. L.; Huffman, J. C. *Science* **1993**, *260*, 1917. (c) Lambert, J. B.; Zhang, S.; Ciro, S. M. *Organometallics* **1994**, *13*, 2430. (d) Lambert, J. B.; Zhang, S. *Science* **1994**, *263*, 986.

(2) Relevant work in this connection has also been published by the following: (a) Xie, Z.; Liston, D. J.; Jelinek, T.; Mitro, V.; Bau, R.; Reed, C. A. *J. Chem. Soc., Chem. Commun.* **1993**, 384. (b) Reed, C. A.; Xie, Z. *Science* **1993**, *263*, 986.

(3) For reviews on silylium cations, see: (a) Lambert, J. B.; Kania, L.; Zhang, S. *Chem. Rev.* **1995**, *95*, 1191 (b) Chojnowski, J.; Stanczyk W.; *Adv. Organomet. Chem.* **1990**, *30*, 243. (c) Chojnowski, J.; Stanczyk, W. *Main Group Chem. News* **1994**, *2*, 6. (d) Lickiss, P. D. *J. Chem. Soc., Dalton Trans.* **1992**, 1333.

(4) (a) Olah, G. A.; Rasul, G.; Li, X.-Y.; Buchholz, H. A.; Sandford, G.; Prakash, G. K. S. *Science* **1994**, *263*, 983. (b) Olah, G. A.; Heiliger, L.; Li, X. Y.; Prakash, G. K. S. *J. Am. Chem. Soc.* **1990**, *112*, 5991. (c) Prakash, G. K. S.; Keyaniyan, S.; Aniszfeld, R.; Heiliger, L.; Olah, G.A.; Stevens, R. C.; Choi, H. K.; Bau, R. *J. Am. Chem. Soc.* **1987**, *109*, 5123. (d) Olah, G. A.; Rasul, G.; Heiliger, L.; Bausch, J.; Prakash, G. K. S. *J. Am. Chem. Soc.* **1992**, *114*, 7737.

(5) Olah, G. A.; Rasul, G.; Buchholz, H. A.; Li, X.-Y.; Prakash, G. K. S. *Bull. Soc. Chim. Fr.* **1995**, *132*, 569.

(6) Olsson, L.; Cremer, D. *Chem. Phys. Lett.* **1993**, *215*, 433.

(7) (a) Olsson, L.; Ottosson, C.-H.; Cremer, D. *J. Am. Chem. Soc.* **1995**, *117*, 7460. (b) Cremer, D.; Olsson, L.; Ottosson, H. *J. Mol. Struct. (THEOCHEM)* **1994**, *313*, 91.

(8) Schleyer, P. v. R.; Buzek, P.; Müller, T.; Apeloig, Y.; Siehl, H.-U. *Angew. Chem.* **1993**, *105*, 1558.

(9) Pauling, L. *Science* **1994**, *263*, 983.

(10) For a description of the NMR/ab initio/IGLO method, see, for example, Cremer, D.; Olsson, L.; Reichel, F.; Kraka, E. *Isr. J. Chem.* **1993**, *33*, 369.

S0276-7333(96)00179-3 CCC: $12.00

Scheme 1

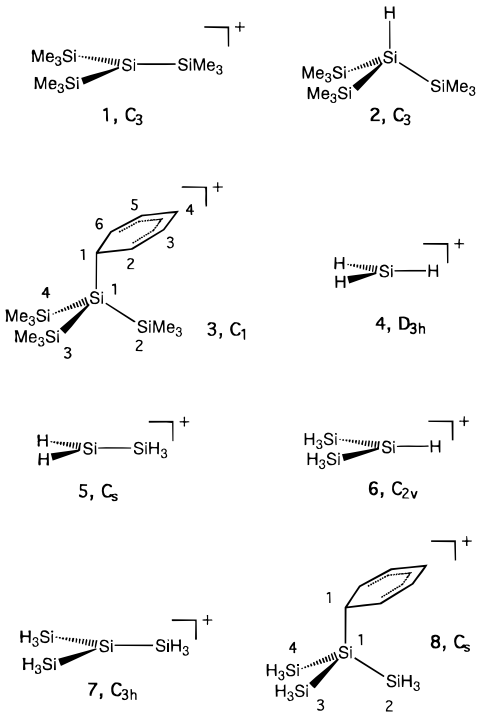

and theoretical shifts not only means a clear identification but also a geometical determination of the molecule in question.[10]

If theoretical and experimental shifts differ considerably, other effects on the molecular geometry have to be considered. For example, we have shown that the properties of $R_3Si(S)^+$ complexes in the gas phase significantly differ from the properties of these complexes in solution.[13] To get reasonable geometries, binding energies, charge distributions, magnetic properties, etc., it is necessary to consider the influence of the surrounding solvent molecules in some way within the ab initio description. In the present work, this is done by placing complex **3** inside an appropriately dimensioned cavity within a polarizable continuum that possesses the same dielectric constant ϵ as benzene. The SCF wave function of **3** in benzene is calculated in a two-step iterative approach where in the second step the buildup of electrostatic charges caused by the electric field of **3** on the surface of the cavity is considered. In this way, the electrostatic impact of the surrounding solvent with dielectric constant ϵ is well represented and major changes in geometry, complex binding energies, charge distribution, and magnetic properties can be calculated. The solvent continuum method used in this work is the PISA approach of Tomasi and co-workers.[14]

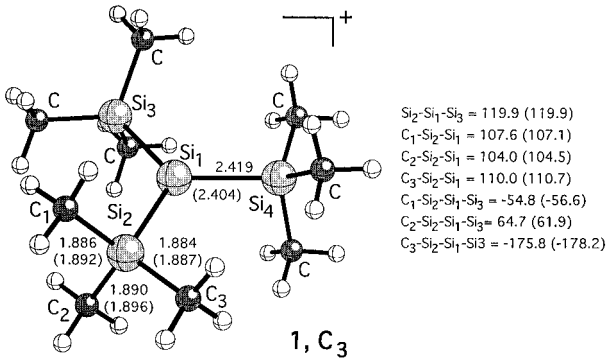

Figure 1. HF/6-31G(d) and B3LYP/6-31G(d) (values in parentheses) geometry of $Si(SiMe_3)_3^+$ (**1**). Relevant geometrical parameters are given in Å (bond lengths) and deg (angles).

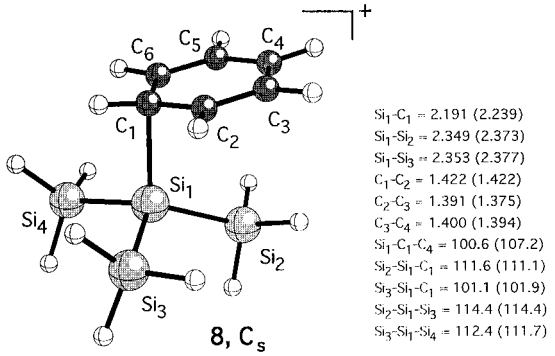

Figure 2. HF/6-31G(d) and MP2/6-31G(d) (values in parentheses) geometry of $Si(SiH_3)_3$-$C_6H_6^+$ (**8**). Relevant geometrical parameters are given in Å (bond lengths) and deg (angles).

Hence, the computational procedure describing the target cation **3** in benzene solution comprised the following steps. First, we carried out geometrical optimizations for molecules **1**−**8** (for symmetry, conformational details, and numbering of atoms, see Scheme 1 and Figures 1, 2, and 3) at the HF level of theory using the 3-21G and 6-31G(d) basis sets.[15] Harmonic frequencies were calculated at HF/3-21G to check that all stationary points calculated correspond to equilibrium geometries. In the second step, NMR chemical shift calculations were performed at HF/6-31G(d) geometries with the IGLO method by Kutzelnigg and Schindler,[16] using a (11s7p2d/9s5p1d/5s1p)[7s6p2d/5s4p1d/3s1p] basis set, which is of TZ+P quality and has been especially designed for ^{13}C and ^{29}Si NMR chemical shift calculations.[16c] In some cases, improved NMR chemical shift calculations were carried out with the GIAO-MP2 method of Gauss,[17] which contrary to IGLO includes pair correlation effects and, therefore, provides a check on possible correlation errors of calculated NMR chemical shifts.

In the third step, the geometry of target cations **1** and **3** was reoptimized with the PISA-HF continuum model using

(11) See, for example, (a) Buzek, P.; Schleyer, P. v. R.; Sieber, S. *Chemie Unserer Zeit* **1992**, *26*, 116. (b) Bühl, M.; Schleyer, P. v. R. In *Electron Deficient Boron and Carbon Clusters*; Olah, G. A., Wade, K., Williams, R. E., Eds.; Wiley: New York, 1991. (c) Bühl, M.; Hommes, N. J. R. v. E.; Schleyer, P. v. R.; Fleischer, U.; Kutzelnigg, W. *J. Am. Chem. Soc.* **1991**, *113*, 2459. (a) Hnyk, D.; Vajda, E.; Buehl, M.; Schleyer, P. v. R. *Inorg. Chem.* **1992**, *31*, 2464. (b) Buehl, M.; Schleyer, P. v. R. *J. Am. Chem. Soc.* **1992**, *114*, 477. (c) Buehl, M.; Schleyer, P. v. R.; McKee, M. L. *Heteroat. Chem.* **1991**, *2*, 499. (d) Buehl, M.; Schleyer, P. v. R. *Angew. Chem.* **1990**, *102*, 962. (e) Schleyer, P. v. R.; Buehl, M.; Fleischer, U. Koch, W. *Inorg. Chem.* **1990**, *29*, 153. (f) Schleyer, P. v. R., Koch, W.; Liu, B.; Fleischer, U. *J. Chem. Soc., Chem. Commun.* **1989**, 1098. (g) Bremer, M.; Schoetz, K.; Schleyer, P. v. R.; Fleischer, U.; Schindler, M.; Kutzelnigg, W.; Koch, W.; Pulay, P. *Angew. Chem.* **1989**, *101*, 1063.

(12) (a) Cremer, D.; Reichel, F.; Kraka, E. *J. Am. Chem. Soc.* **1991**, *113*, 9459. (b) Cremer, D.; Svensson, P.; Kraka, E.; Ahlberg, P. *J. Am. Chem. Soc.* **1993**, *115*, 7445. (c) Cremer, D.; Svensson, P.; Kraka, E.; Konkoli, Z.; Ahlberg, P. *J. Am. Chem. Soc.* **1993**, *115*, 7457. (d) Sieber, S.; Schleyer, P. v. R.; Otto, A. H.; Gauss, J.; Reichel, F.; Cremer, D. *J. Phys. Org. Chem.* **1993**, *6*, 445. (e) Szabo, K.; Cremer. D. *J. Org. Chem.*, in press. (f) Cremer, D.; Childs, R. F.; Kraka, E. In *The Chemistry of the Cyclopropyl Group*; Rappoport, Z., Ed.; Wiley Interscience: New York, 1995; Vol. 2 p 339. (g) Childs, R. F.; Cremer, D.; Elia, G. In *The Chemistry of the Cyclopropyl Group*; Rappoport, Z., Ed.; Wiley Interscience: New York, 1995; Vol. 2 p 411.

(13) Arshadi, M.; Johnels, D.; Edlund, U.; Ottosson, C.-H.; Cremer, D. *J. Am. Chem. Soc.* **1996**, *118*, 5120.

(14) (a) Miertus, S.; Scrocco, E.; Tomasi, *J. Chem. Phys.* **1981**, *55*, 117. (b) Pascual-Ahuir, J. L.; Silla, E.; Tomasi, J.; Bonaccorsi, R. *J. Comput. Chem.* **1987**, *8*, 778.

(15) (a) Binkley, J. S.; Pople, J. A.; Hehre, W. J. *J. Am. Chem. Soc.* **1980**, *102*, 939. (b) Gordon, M. S.; Binkley, J. S.; Pople, J. A.; Pietro, W. J.; Hehre, W. J. *J. Am. Chem. Soc.* **1982**, *104*, 2797. (c) Hariharan, P. C.; Pople, J. A. *Theor. Chim. Acta* **1973**, *28*, 213.

(16) (a) Kutzelnigg, W. *Isr. J. Chem.* **1980**, *19*, 193. (b) Schindler, M.; Kutzelnigg, W. *J. Chem. Phys.* **1982**, *76*, 1919. (c) Kutzelnigg, W.; Schindler, M.; Fleicher, U. *NMR, Basic Principles and Progress*; Springer: Berlin, 1990; Vol. 23, p 1.

(17) (a) Gauss, J. *Chem. Phys. Lett.* **1992**, *191*, 614. (b) Gauss, J. *J. Chem. Phys.* **1993**, *99*, 3629.

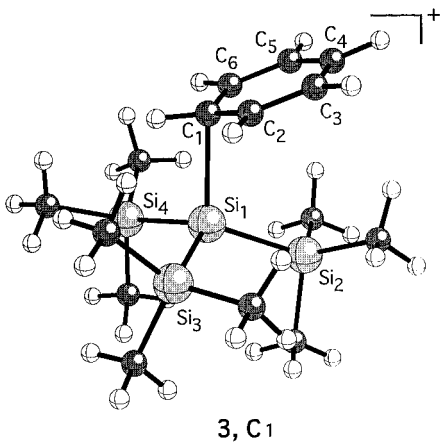

Figure 3. NMR/ab initio/IGLO geometry of Si(SiMe$_3$)$_3$-C$_6$H$_6^+$ (**3**) based on PISA and SCRF/6-31G(d) calculations carried out at the HF level. The geometry corresponds to the experimental ^{29}Si NMR shift value of 111 ppm[1a,b] measured for **1** in benzene solution. The gas phase geometry calculated at the B3LYP/6-31G(d) level is given in parentheses. Relevant geometrical parameters are given in Å (bond lengths) and deg (angles).

the dielectric constant of benzene ($\epsilon = 2.27$).[18] Test calculations revealed that the most sensitive parameter of **3** is the Si1−C1 distance while all other geometrical parameters change in relation to this distance. Geometrical optimizations with the PISA approach are rather costly since they have to be done numerically. Therefore, only the most critical geometrical parameters were optimized at the PISA level while the rest of the molecule was determined using the self-consistent reaction field (SCRF) model.[19] This approach leads to geometries identical with the true PISA/6-31G(d) geometry within 0.001 Å and 0.1°. The PISA/6-31G(d) geometry obtained in this way for cation **3** was used to determine IGLO NMR chemical shift values for **3** in benzene solution.

In the final step, the NMR/ab initio/IGLO approach was applied by determining that PISA/6-31G(d) geometry which leads to an exact reproduction of experimental NMR chemical shift values, i.e., the $\delta(^{29}\text{Si})$ value of the central Si atom, by calculated IGLO NMR chemical shifts. This geometry is the NMR/ab initio/IGLO geometry which is considered to represent the true molecular geometry of **3** in benzene solution[10−12], and therefore, all properties of the cation reported in this work were evaluated for this geometry.

Since the NMR/ab initio/IGLO geometry covers both correlation and solvent effects on the geometry, we separated the two effects by also carrying out DFT calculations at the B3LYP/6-31G(d) level.[20] Test calculations on small silylium cations suggest that B3LYP covers major correlation effects thus leading to geometries and complexation energies of MP2 or even higher quality. By comparing HF, PISA, and B3LYP results, we can predict the joint effect of correlation corrections and solvent effects and compare them with the NMR/ab initio/IGLO results.

At the final NMR/ab initio/IGLO geometry, the electron density distribution $\rho(\mathbf{r})$ was analyzed using the virial partitioning method of Bader and co-workers.[21] From this analysis, the character of a certain bond can be classified as covalent or noncovalent according to criteria given by Cremer and Kraka.[22] These authors have given two conditions for the existence of a covalent bond between two atoms A and B. (1) Atoms A and B have to be connected by a path of maximum electron density (MED path). The existence of such a MED path implies a (3, −1) saddle point $\mathbf{r_b}$ of the electron density distribution $\rho(\mathbf{r})$ as well as a zero-flux surface between A and B (necessary condition). (2) The local energy density $H(\mathbf{r_b})$ has to be stabilizing, i.e., it must be smaller than zero (sufficient condition). These two criteria have helped to distinguish covalent bonding from noncovalent, ionic, or electrostatic interactions in many cases and to characterize covalent bonding in molecules with both classical and nonclassical structures.[23,24]

Calculations were performed on a CRAY YMP-464 and a SGI Power Challenge using the ab initio program packages COLOGNE 96,[25] GAUSSIAN 92,[26] and ACES II.[27]

3. Results and Discussion

Relevant parameters of the calculated geometries of **1**, **3**, and **8** are given in Figures 1, 2, and 3 as well as in Table 1. Cartesian coordinates and the corresponding energies are listed in the Supporting Information. Calculated NMR chemical shifts for molecules **1**−**8** are summarized in Table 2.

Olah and co-workers[5] calculated for cation **7** a $\delta(^{29}\text{Si})$ chemical shift value of 865.7 ppm at the IGLO/[7s6p2d/5s4p1d/2s] level of theory (DZ quality of the H basis because of computational reasons), which is downfield by 1005 ppm from the corresponding value (−139.2 ppm) of the parent silane HSi(SiH$_3$)$_3$. These values are confirmed at the IGLO/[7s6p2d/5s4p1d/3s1p] level (TZ+P quality of the H basis, Table 2). A large downfield shift of 1040 ppm as compared to the $\delta(^{29}\text{Si})$ chemical shift value of the parent silane **2** ($\delta(^{29}\text{Si}) = -120$ ppm, Table 2) is also calculated for cation **1** ($\delta(^{29}\text{Si}) = 920$ ppm). The fact that calculated and experimental shift values ($\delta(^{29}\text{Si}) = -117$ ppm) [1a] for **2** are in good agreement may suggest also some reliability of the calculated value of

(18) *Handbook of Chemistry and Physics*; 64th and 72nd eds.; Lide, D. R., Ed.; CRC Press: Boca Raton, FL, 1983 and 1991.

(19) (a) Wong, M. W.; Frisch, M. J.; Wiberg, K. B. *J. Am. Chem. Soc.* **1991**, *113*, 4776. (b) Wong, M. W.; Wiberg, K. B.; Frisch, M. J. *J. Am. Chem. Soc.* **1992**, *114*, 523. (c) Wong, M. W.; Wiberg, K. B.; Frisch, M. J. *J. Am. Chem. Soc.* **1992**, *114*, 1645.

(20) (a) Becke, A. D. *J. Chem. Phys.* **1993**, *98*, 5648. (b) Stevens, P. J.; Devlin, F. J.; Chablowski, C. F.; Frisch, M. J. *J. Phys. Chem.* **1994**, *98*, 11623.

(21) (a) Bader, R. F. W.; Nguyen-Dang, T. T.; Tal, Y. *Rep. Prog. Phys.* **1981**, *44*, 893. (b) Bader, R. F. W.; Nguyen-Dang, T. T. *Adv. Quantum Chem.* **1981**, *14*, 63.

(22) (a) Cremer, D.; Kraka, E. *Croat. Chem. Acta* **1984**, *57*, 1259. (b) Cremer, D.; Kraka, E. *Angew. Chem., Int. Ed. Engl.* **1984**, *23*, 62.

(23) (a) Kraka, E.; Cremer, D. In *Theoretical Models of the Chemical Bond;* Maksic, Z. B., Ed.; Springer: Berlin, 1990; Part 2 (The Concept of the Chemical Bond), p 453. (b) Cremer, D. In *Modelling of Structure and Properties of Molecules;* Maksic, Z. B., Ed.; Ellis Horwood: Chichester, England, 1988; p 125. (c) Cremer, D.; Kraka, E. In *Molecular Structure and Energetics, Structure and Reactivity;* Liebman, J. F., Greenberg, A., Eds.; VCH Publishers: New York, 1988; Vol. 7, p 65. (d) Cremer, D. *Tetrahedron* **1988**, *44*, 7427.

(24) (a) Cremer, D.; Gauss, J.; Schleyer, P. v. R.; Budzelaar, P. H. M. *Angew. Chem., Int. Ed. Engl.* **1984,** *23*, 370. (c) Cremer, D.; Kraka, E. *J. Am. Chem. Soc.* **1985**, *107*, 3800, 3811. (d) Cremer, D.; Gauss, J. *J. Am. Chem. Soc.* **1986**, *108*, 7467. (e) Cremer, D.; Bock, C. W. *J. Am. Chem. Soc.* **1986,** *108*, 3375. (f) Koch, W.; Frenking, G.; Gauss, J.; Cremer, D.; Sawaryn, A.; Schleyer, P. v. R. *J. Am. Chem. Soc.* **1986**, *108*, 5732. (g) Koch, W.; Frenking, G.; Gauss, J.; Cremer, D. *J. Am. Chem. Soc.* **1986**, *108*, 5808. (h) Budzelaar, P. H. M.; Cremer, D.; Wallasch, M.; Würthwein, E-U.; Schleyer, P. v. R. *J. Am. Chem. Soc.* **1987**, *109*, 6290. (i) Koch, W.; Frenking, G.; Gauss, J.; Cremer, D.; Collins, J. R. *J. Am. Chem. Soc.* **1987**, *109*, 5917. (j) Cremer, D.; Gauss, J.; Kraka, E. *J. Mol. Struct. (THEOCHEM)* **1988**, *169*, 531. (k) Frenking, G.; Koch, W.; Reichel, F.; Cremer, D. *J. Am. Chem. Soc.* **1990**, *112*, 4240.

(25) Kraka, E.; Gauss, J.; Reichel, F.; Olsson, L.; Zhi He, Konkoli, Z.; Cremer, D. *Cologne 96*; University of Göteborg: Sweden, 1996.

(26) *Gaussian 92*; Frisch, M. J.; Head-Gordon, M.; Trucks, G. W.; Foresman, J. B.; Schlegel, H. B.; Raghavachari, K.; Robb, M. A.; Binkley, J. S.; Gonzalez, C.; Defrees, D. J.; Fox, D. J.; Whiteside, R. A.; Seeger, R.; Melius, C. F.; Baker, J.; Martin, R. L.; Kahn, L.R.; Stewart, J. J. P.; Topiol, S.; Pople, J. A. *Gaussian 92*; Gaussian Inc.: Pittsburgh, PA, 1992.

(27) Stanton, J. F.; Gauss, J.; Watts, J. D.; Lauderdale, W. J.; Bartlett, R. J. *ACES II*; Quantum Theory Project: University of Florida, Gainesville, 1992.

Table 1. Geometry of 3 in Gas and Solution Phase[a]

	gas phase		solution[b]	
geometry parameter	HF/ 6-31G(d)	B3LYP/ 6-31G(d)	PISA/ 6-31G(d)	NMR/ ab initio/IGLO
Si1−C1	2.452	2.378	2.369	2.293
Si1-Si2	2.409	2.403	2.409	2.409
Si1-Si3	2.413	2.409	2.412	2.413
Si1-Si4	2.417	2.414	2.417	2.417
C1−C2	1.410	2.421	2.412	1.417
C2−C3	1.377	1.389	1.377	1.375
C3−C4	1.392	1.402	1.393	1.393
C4−C5	1.388	1.399	1.389	1.390
C5−C6	1.382	1.391	1.381	1.379
C6−C1	1.407	1.420	1.409	1.414
H−C1	1.078	1.090	1.079	1.080
Si2−Si1−Si3	115.2	114.8	115.0	114.2
Si2−Si1−Si4	114.9	114.8	114.6	113.9
Si3−Si1−Si4	112.4	112.1	112.1	111.3
Si2−Si1−C1	112.2	112.5	112.5	113.1
Si3−Si1−C1	99.5	99.4	100.0	101.0
Si4−Si1−C1	100.5	101.4	100.8	101.7
Si1−C1−C4	110.5	111.6	110.8	112.5
H−C1−C4	84.8	85.4	85.5	87.1
H−C1−C4	164.7	163.0	163.8	160.5
Si2−Si1−C1−C4	−7.0	−3.9	−7.3	−6.8
Si3−Si1−C1−C4	115.4	118.1	115.4	116.6
Si4−Si1−C1−C4	−129.5	−127.0	−129.6	−128.5
Si2−Si1−C1−H	172.7	175.7	172.7	173.7
Si3−Si1−C1−H	−65.0	−62.4	−64.9	−63.7
Si4−Si1−C1−H	50.1	52.6	50.1	51.1

[a] Bond lengths in Å, angles in deg. [b] Calculated for a benzene solution with $\epsilon = 2.27$.

1. On the other hand, downfield shifts of 1000 ppm and more have not been found for any other silylium cation.

If one takes the $\delta(^{29}Si)$ chemical shift values of $(Me_3Si)_3SiH$, SiH_4, and SiH_3^+ and assumes that a $SiMe_3$ substituent leads to the same changes of $\delta(^{29}Si)$ for silane and associated silylium cation, a shift value of 250 rather than 920 ppm can be predicted for **1**.[6] Therefore, the accuracy of the IGLO method has to be questioned in the case of silyl-substituted silylium cations. This is particularly important in the present case since the characterization of the silylium cation character of **1** or **7** in benzene solution is primarily based on the $\delta(^{29}Si)$ shift value in the gas phase, which is only available from ab initio calculations. If for **1** this value would be just 250 ppm, a measured $\delta(^{29}Si) = 111$ ppm for **1** in benzene[1] would suggest a high degree of silylium cation character while a value of 920 ppm suggests almost none of it.

To verify the reliability of calculated NMR chemical shift values, the GIAO-MP2 method was used for a MP2/6-31G(d) geometry of **7**. The GIAO-MP2 $\delta(^{29}Si)$ value (930 ppm relative to SiH_4; GIAO-SCF: 883 ppm) is 47 ppm more downfield than the GIAO-SCF value. Downfield shifts by 30−40 ppm have also been obtained for the $\delta(^{29}Si)$ values of alkyl-substituted silylium ions at GIAO-MP2 level.[7] The true $\delta(^{29}Si)$ value should actually appear slightly more upfield since GIAO-MP2 is known to somewhat overestimate correlation effects.[28] In any case, GIAO-MP2 confirms IGLO-HF results for the ^{29}Si shifts of uncoordinated **1** and **7** in the gas phase.

In general, the downfield shifts of planar silylium cations are caused by paramagnetic currents in the plane of the σ-bonds.[16c] The paramagnetic contribution to the chemical shift value is irreversibly proportional to the sum of differences between ground state energy and the energies of excited electronic states. The largest paramagnetic contribution is associated with energy differences between ground state and the lowest excited states which can be estimated from the energy differences between the frontier orbitals (HOMO, sub-HOMO, LUMO, etc.) In the case of SiR_3^+ ions , the LUMO largely corresponds to the empty $3p\pi(Si)$ orbital mixed with small contributions of the pseudo-π(R) orbitals of the attached alkyl or silyl groups while HOMO and sub-HOMOs correspond to the in-plane pseudo-$\pi(SiR_3)$ and out-of-plane pseudo-π(R) orbitals where the latter may contain some admixture of the $3p\pi(Si)$ orbital because of hyperconjugation. The large downfield ^{29}Si shifts for cations **1** and **7** (Table 2) can be explained as a result of enhanced paramagnetic ring currents indicated by relatively small HOMO−LUMO gaps.

In Figure 4, IGLO $\delta(^{29}Si)$ values (central Si nucleus) of molecules $SiH_{3-n}(SiH_3)_n^+$ (**4**−**7**) are plotted vs the number n of SiH_3 groups attached to the central Si atom and compared with the corresponding dependence of $\delta(^{29}Si)$ on the number of CH_3 groups in the case of cations $SiH_{3-n}(CH_3)_n^+$. In both cases, $\delta(^{29}Si)$ depends linearly on n; however, $\delta(^{29}Si)$ values for cations $SiH_{3-n}(SiH_3)_n^+$ vary by 600 ppm between 270 and 870 ppm while those of cations $SiH_{3-n}(CH_3)_n^+$ vary by just 60 ppm.

The relationship between the difference ϵ(LUMO) − ϵ(HOMO), i.e., the HOMO−LUMO gap, and n is given in Figure 5. For cations $SiH_{3-n}(CH_3)_n^+$, the HOMO−LUMO gap is relatively large and changes little with n. As a consequence, paramagnetic currents for these ions are small leading to a downfield shift of about 300 ppm. However, for cations $SiH_{3-n}(SiH_3)_n^+$ the HOMO−LUMO gap decreases exponentially with n and adopts a relatively small value for $n = 3$. Accordingly, paramagnetic currents strongly increase with the number n of SiH_3 groups leading to a downfield shift of more than 1000 ppm in the case of **7**.

These trends can be understood when considering (a) the inductive effect of substituent R (related to the group electronegativity of R relative to that of Si^+) and (b) hyperconjugative interactions of the out-of-plane pseudo-π MOs with the $3p\pi(Si^+)$ orbital.

In the series R = H, CH_3, and SiH_3, electropositive character increases, which leads to a rise of the energies of the HOMO and sub-HOMOs thus decreasing the HOMO−LUMO gap and the lowest excitation energies. Hyperconjugative interactions between the out-of-plane pseudo-π MOs and the $3p\pi(Si^+)$ orbital will raise the energy of the LUMO, and although hyperconjugative effects are much smaller than inductive effects, they will partially cancel changes in the HOMO−LUMO gap due to inductive effects. Clearly, hyperconjugative interactions are stronger in $SiH_{3-n}(CH_3)_n^+$ than in $SiH_{3-n}(SiH_3)_n^+$ since the shorter Si−C bond leads to larger overlap between the orbitals involved. When all H atoms in SiH_3^+ were replaced stepwise by CH_3, the HOMO−LUMO gap decreases slowly (Figure 5) because of opposing inductive and hyperconjugative effects.

For $SiH_{3-n}(SiH_3)_n^+$, inductive effects (caused by the electropositive character of SiH_3) are significantly larger than hyperconjugative effects, and therefore, the

(28) (a) Gauss, J.; Stanton, J. *J. Chem. Phys.* **1995**, *102*, 251. (b) Gauss, J.; Stanton, J. *J. Chem. Phys.* **1995**,*103*, 3561.

Table 2. IGLO/[7s6p2d/5s4p1d/3s1p]//HF/6-31G(d) ^{29}Si and ^{13}C NMR Chemical Shifts (Relative to TMS) of 1−8 Calculated at HF/6-31G(d) Geometries (Gas Phase) or NMR/ab Initio/IGLO-PISA/6-31G(d) Geometries (3, Solution Phase)

		$\delta(^{29}Si)$		
molecule	sym	central Si	silyl Si [b]	$\delta(^{13}C)$[c]
1, Si(SiMe$_3$)$_3^+$	C_3	920.4	8.5	−3.7; −1.0
2, SiH(SiMe$_3$)$_3$	C_3	−119.6 −117.4[a]	−13.4	0.3; 1.3
3, Si(SiMe$_3$)$_3$−C$_6$H$_6^+$	C_1			
gas phase		205.8	−4.1; −3.5	96.0; 158.4; 134.9; 158.9; 136.3; 158.2
benzene solution		111.1[a]	−5.0; −5.8	88.2; 167.5; 134.1; 164.4; 135.2; 166.5
4, SiH$_3^+$	D_{3h}	270.2		
5, SiH$_2$SiH$_3^+$	C_s	433.1	−83.3	
6, SiH(SiH$_3$)$_2^+$	C_{2v}	642.3	−79.2	
7, Si(SiH$_3$)$_3^+$	C_{3h}	868.1	−75.8	
8, Si(SiH$_3$)$_3$−C$_6$H$_6^+$[d]	C_s	55.6; *27.8*	*−97.1; −84.0*	89.8; 170.4; 139.7; 166.4; 139.7; 170.4

[a] Experimental value from ref 1. [b] In case of two entries, the lower and upper shift values are always given. [c] For the benzenium rings, shift values are given according to the numbering shown in Scheme 1. [d] Reference 5. Values in italics refer to ^{29}Si shifts calculated at MP2/6-31G(d) geometries (this work).

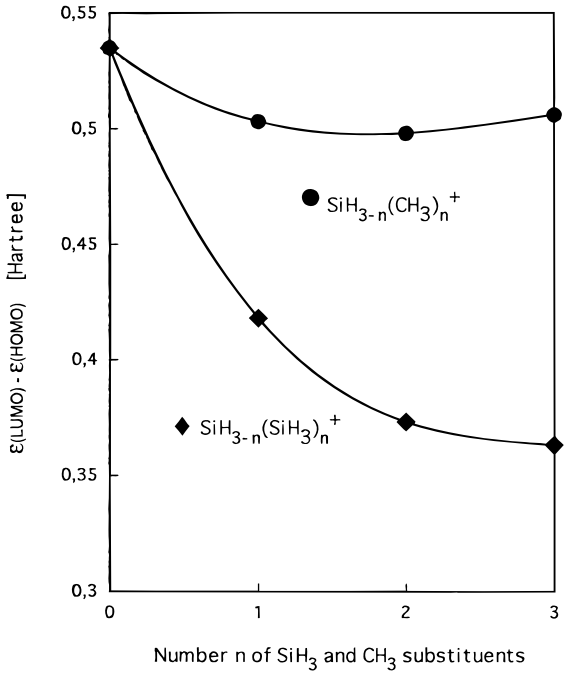

Figure 4. Dependence of the $\delta(^{29}Si)$ value of the central Si atom in cations SiH$_{3-n}$(SiH$_3$)$_n^+$ (**4**−**7**) and SiH$_{3-n}$(CH$_3$)$_n^+$ on the number n of SiH$_3$ or CH$_3$ substituents.

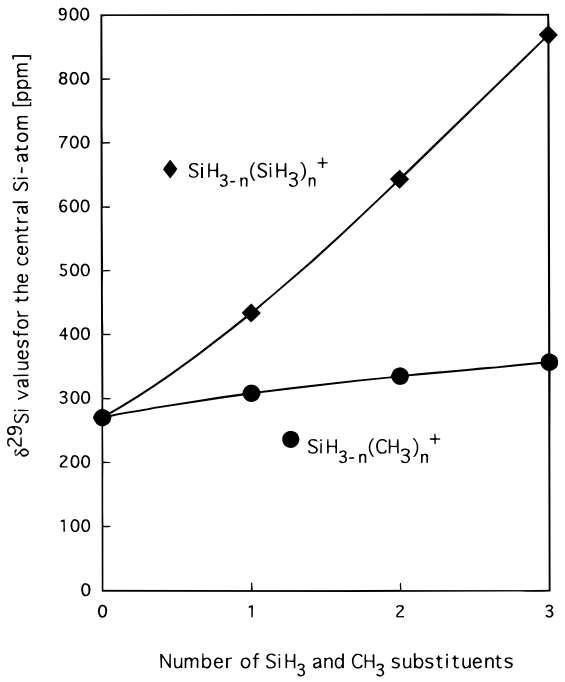

Figure 5. Dependence of the HOMO−LUMO gap $\Delta\epsilon = \epsilon(\text{LUMO}) - \epsilon(\text{HOMO})$ in cations SiH$_{3-n}$(SiH$_3$)$_n^+$ (**4**−**7**) and SiH$_{3-n}$(CH$_3$)$_n^+$ on the number n of SiH$_3$ or CH$_3$ substituents. $\Delta\epsilon$ from HF/[7s6p2d/5s4p1d/3s1p]//HF/6-31G(d) calculations.

HOMO−LUMO gap, as well as the lowest excitation energies, decreases strongly with n. As a consequence, the paramagnetic (deshielding) contributions to $\delta(^{29}Si)$ of the central Si atom are much stronger and, accordingly, lead to downfield shifts up to 1000 ppm and more.

In conclusion, we can say that the calculated difference of 1040 ppm in $\delta(^{29}Si)$ values for **1** and **2** (Table 2) is reasonable and a consequence of the electronic nature of three silyl substituents SiR$_3$. Furthermore, it is in line with the calculated downfield shift of **7** (1005 ppm) since the HOMO−LUMO gaps for **1** and **7** are 0.339 and 0.363 hartree. In view of the fact that Lambert and coworkers measured a $\delta(^{29}Si)$ value of just 111 ppm for **1** in benzene solution, which corresponds to about 22% of the calculated downfield shift of the $\delta(^{29}Si)$ value of **1** in the gas phase, little silylium cation character should be expected for **1** in solution. Solvent coordination and the formation of a Wheland σ-complex, **3**, are most likely.

Complex **3** has C$_1$ symmetry and at the HF/6-31G(d) level a Si1−C1 bond length of 2.45 Å (Table 1). The bond length is longer than the bond lengths in other complexes between SiR$_3^+$ and aromatic solvent molecules (2.13−2.29 Å)[5,6,8] investigated at the same level of theory. Also, the calculated coordination energy of 9.6 kcal/mol is smaller than any of the previously reported values for complexes SiR$_3$−ArylH$^+$.[5,6,8] For example, for **8**, the coordination energy is 24.2 kcal/mol. This is in line with a much shorter Si−C distance (2.24 Å) and a significantly shielded ^{29}Si shift value of 55.6 ppm.[5]

The MP2/6-31G(d) geometry optimization of **8** leads to a geometry (Figure 2) that is characterized by a Si1−C1 distance of 2.191 Å, which is shorter by 0.048 Å compared to the corresponding HF/6-31G(d) distance (2.239 Å, Figure 2). Similar shortenings of Si−X distances in silylium cation−solvent complexes at MP2 have been observed by other authors,[4,8] and therefore, it was necessary to calculate the gas phase geometry of **3** also at a correlation corrected level of theory. For this

purpose, B3LYP was used since this approach is less costly than MP2 and covers (in an unspecified way) also higher correlation effects than the MP2 approach.

The B3LYP/6-31G(d) geometry optimization of **3** leads to a much shorter Si1−C1 distance (2.38 Å, Table 1, Figure 3) than that calculated at HF while all other geometrical parameters change only slightly compared to those of the HF geometry (SiC bond lengths become 0.003−0.006 Å shorter and CC bond lengths 0.01 Å longer). The decrease of the Si1−C1 distance by 0.07 Å results from the fact that correlation increases the electron density between Si1 and C1 thus strengthening the coordination of benzene to **1**, which is confirmed by an increase in the complexation energy from 9.6 (HF) to 14.3 kcal/mol (B3LYP). However, this is still 10 kcal/mol smaller than the complexation energy of **8**.

The differences between **3** and **8** are a consequence of electronic differences and differences in steric demand between $-SiH_3$ and $-SiMe_3$ substituents. Because of the larger electronegativity of the latter substituent ($\chi(H) = 7.18 < \chi(CH3) = 7.45$ hence $\chi(SiH_3) < \chi(SiMe_3)$[29]), the positive charge is larger for the central Si atom of **1** (0.057 e) than that for **7** (−0.035 e) at HF/TZ+P//HF/6-31G(d) level; however, this is of secondary importance (only causing a contraction of the 3pπ(Si) orbital) since the availability of the 3pπ(Si) orbital primarily determines coordination with a benzene molecule. In **1**, hyperconjugative interactions lead to an energy rise of the LUMO, which therefore is less available for bonding interactions between silylium cation and benzene in complex **7**.

The amount of steric hindrance caused by a certain substituent R is obtained via its *A* value, derived from the axial−equatorial equilibria in cyclohexyl-R derivatives.[30] A higher *A* value for $SiMe_3$ (3.41 kcal/mol) than for SiH_3 (1.26 kcal/mol) has been reported.[31] Accordingly, both hyperconjugative effects and the larger steric demand of a $SiMe_3$ group should make coordination weaker in **3** than in **8**.

For the central Si atom in **3**, the IGLO $\delta(^{29}Si)$ value is 206 ppm, which is 95 ppm downfield of the experimental value of 111 ppm. This difference suggests that solvent−solute interactions have a strong influence on the nature of **3** and that calculations including solvent effects are necessary to get a reliable description. When the geometrical optimization of **3** was repeated with the PISA continuum model using the dielectric constant of benzene ($\epsilon = 2.27$[18]), the Si1−C1 bond length decreases by 0.08 Å from 2.45 to 2.37 Å while only relatively small changes are observed for all other geometrical parameters. The decrease of the Si1−C1 interaction distance in solution is typical of silylium cation−solvent complexes $R_3Si(S)^+$ and is due to the electrostatic interactions between $R_3Si(S)^+$ and the surrounding media S.[13] They facilitate a larger charge transfer from S to R_3Si^+ and, by this, stronger binding interactions between S and the silylium cation. Parallel to the decrease in the Si1−C1 distance, the $\delta(^{29}Si)$ shift value of Si1 decreases by 52 ppm to 154 ppm, which is in better agreement with the experimental value, although it is still 43 ppm too large.

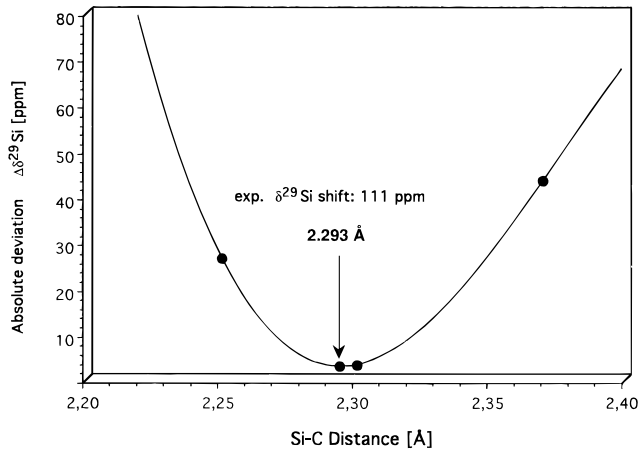

Figure 6. Determination of the Si−$C_{benzene}$ distance in $Si(SiMe_3)_3$-$C_6H_6^+$ (**3**) with the help of the NMR/ab initio/IGLO method. Absolute deviation $\Delta\delta(^{29}Si)$ between experimental and calculated $\delta(^{29}Si)$ shifts are in ppm.

Both correlation and solvent effect lead to a decrease of the Si1−C1 distance while all other geometrical parameters are only slightly changed by these effects. Assuming that the correlation effect (0.074 Å) and the solvent effect (0.083 Å) for distance Si1−C1 are additive (0.175 Å), one can predict a Si1−C1 distance of 2.295 Å for **3** in benzene solution. Similarly, the complexation energy for **3** can be estimated to be 9.6 + 4.7−0.5 = 13.8 kcal/mol. Direct confirmation of these predictions requires a PISA-MP2 method with analytical gradients for geometrical optimization, which is presently not available.

In this situation, we used the NMR/ab initio/IGLO approach and determined with PISA and SCRF the geometry that reproduces the experimental $\delta(^{29}Si)$ value of 111 ppm for complex **3** (compare with Figure 6). This geometry is shown in Figure 3. It is characterized by a Si1−C1 interaction distance of 2.293 Å, which is 0.09 Å shorter than the B3LYP gas phase value of 2.38 Å (Table 1) and agrees well with the predicted value of 2.295 Å. The corresponding complex binding energy is 13.6 kcal/mol**.** Hence, the NMR/ab initio/IGLO approach leads to a reasonable description of **3** at a relatively low cost level.

The geometry of **3** resembles that of the $Si(Me)_3-C_6H_6^+$ complex. In both cases, one substituent is placed below the benzene ring while the other two substituents adopt an exo position. In this way, steric repulsion between the benzene ring and the substituents R is minimized, although this requires some significant geometrical changes in the case of **3** because of the steric bulk of three $SiMe_3$ groups. For example, the angle Si1−C1−C4, which is a measure for the backfolding of the benzene ring, increases from 107.6 to 112.5° when replacing Me groups in $Si(Me)_3-C_6H_6^+$ by $SiMe_3$ groups. Similarly, the Si2−Si1−C1 angle increases from 109.4 to 113.1° (Figure 3) and the Si1−C1 distance from 2.21 to 2.293 Å where one should actually consider the gas phase value of **3** (2.45 Å) since the geometry of $Si(CH_3)_3-C_6H_6^+$ has only been calculated for the gas phase.[6] These geometrical deviations between **3** and $Si(CH_3)_3-C_6H_6^+$ guarantee that the closest H−H contacts in **3** (2.27−2.6 Å) are within 10% of the optimal van der Waals H−H distance of 2.4 Å.[18]

(29) Bergmann, D.; Hinze, J. T. *Struct. Bonding* **1987**, *66*, 145.
(30) Eliel, E. L.; Wilen, S. H.; Mander, L. N. *Stereochemistry of Organic Compounds*; Wiley: New York, 1994.
(31) Frey, J.; Schottland, E.; Rappoport, Z.; Bravo-Zhivotovskii, D.; Nakash, M.; Botoshansky, M.; Kaftory, M.; Apeloig, Y. *J. Chem. Soc., Perkin Trans. 2* **1994**, 2555 and references therein.

The geometry given in Figure 3 presents the geometry of the Wheland σ-complex formed when **1** is dissolved in benzene. Even though benzene is a relatively weak nucleophile, interactions with benzene are significant. A charge transfer of 0.31 e, calculated from Mulliken charges, is similar to that found in other $SiR_3-C_6H_6^+$ complexes.[6,7] Furthermore, the properties of the electron density distribution $\rho(\mathbf{r})$ between Si1 and C1 suggest the formation of a weak covalent bond according to the criteria given by Cremer and Kraka.[22] There is a path of maximum electron density connecting Si1 and C1 with a bond critical point $\mathbf{r}_b$ between these atoms. At $\mathbf{r}_b$, the electron density $\rho(\mathbf{r}_b)$ is 0.28 Å^{-3} and the energy density $H(\mathbf{r}_b)$ is −0.11 hartree Å^{-3}. The bond energy of the bond Si1−C1 should be directly related to the complexation energy of about 14 kcal/mol. The formation of a weak covalent bond distorts the central Si atom from tri- toward tetravalency as indicated by bond angles C1−Si1−Si of 101, 102, and 113° (Figure 3). It also causes alternations in the C−C bond lengths of the benzene ring (1.375−1.417 Å, Figure 3). The positive charge is clearly delocalized over the benzene ring indicating that **3** has to be considered as a silyl−benzenium cation rather than a silylium cation.

Conclusions

Using the NMR/ab initio/IGLO method, the nature of **1** in benzene is identified as that of a Wheland σ-complex, **3**, formed by electrophilic substitution of the benzene ring by **1**. There is a weak covalent Si1−C1 bond between **1** and the benzene ring leading to a tetravalent Si atom. Charge delocalization and Si1−C1 bond indicate a loss of silylium cation character. In the gas phase, Si1−C1 bonding in **3** is weaker than in any other $SiR_3-C_6H_6^+$ σ-complex so far investigated. This is reflected by a B3LYP complexation energy of 14.3 kcal/mol and a rather long Si1−C1 distance of 2.38 Å . However, electrostatic interactions between **3** and the solvent shell in benzene reduce the Si1−C1 bond length considerably. According to the NMR/ab initio/IGLO approach used in this work, complexation energy and Si1−C1 bond distance of **3** in benzene solution are 13.6 kcal/mol and 2.293 Å, respectively.

The confusion about the alleged silylium cation character of **1** in benzene solution could be solved in this work by calculating the $\delta(^{29}Si)$ chemical shift of **1** in the gas phase to be 920 ppm rather than 250 ppm as previously estimated. [6] The unusually positive $\delta(^{29}Si)$ values of trisilyl-substituted silylium ions result from large paramagnetic shift contributions due to low-lying excited states as indicated by relatively small HOMO−LUMO gaps.

The expectation that the bulky $SiMe_3$ groups may block any close approach of aromatic solvent molecules to a silylium cation has been shattered by these results. The three $SiMe_3$ groups can be sufficiently bent backward to give the benzene ring enough space for a close contact with the central Si atom. Steric strain is avoided by many small changes in the geometry of the substituents (SiSi bond lengthening, rotations of the methyl groups). From this it becomes clear that steric blocking of a silylium cation from any interactions with an aromatic solvent molecule requires more rigid substituents R than provided by the trimethylsilyl groups.

Acknowledgment. This work was supported by the Swedish Natural Science Research Council (NFR). The calculations were done on the Cray-YMP/416 computer of the Nationellt Superdatorcentrum (NSC), Linköping, Sweden, as well as on the SGI Power Challenge of the MEDNET Computer Laboratory, Göteborg University, Sweden. The authors thank both the NSC and MEDNET for a generous allotment of computer time.

Supporting Information Available: A listing of Cartesian coordinates of all optimized geometries calculated in this work and ball-and-stick representations of these geometries (12 pages). Ordering information is given on any current masthead page.

OM960179F